Dynamics and Control of Shock Shells in the Coulomb Explosion of Very Large Deuterium Clusters

F. Peano,[1,2] R. A. Fonseca,[1] and L. O. Silva[1,*]

[1]GoLP/Centro de Física dos Plasmas, Instituto Superior Técnico, 1049-001 Lisboa, Portugal
[2]I.N.F.M. and Dipartimento di Energetica, Politecnico di Torino, corso Duca degli Abruzzi 24, 10129 Torino, Italy

(Received 21 April 2004; published 25 January 2005)

The explosion dynamics of very large ($\sim 10^6$–10^7 atoms) deuterium clusters irradiated by ultraintense laser pulses ($I \sim 10^{18}$ W/cm^2) is analyzed self-consistently with one-to-one three-dimensional and two-dimensional fully relativistic particle-in-cell simulations. Small-scale shock shells in the expanding ion cloud are observed. A technique to induce the formation of large shock shells inside a single cluster, increasing the probability of intracluster nuclear reactions, is proposed and demonstrated.

DOI: 10.1103/PhysRevLett.94.033401 PACS numbers: 36.40.Gk, 52.65.Rr

The interaction of ultraintense ($I > 10^{16}$ W/cm^2) and ultrafast (duration $\sim$10–100 fs) laser pulses with clustered gases is a central research topic [1–6]. In these targets, almost 100% of the laser energy is transferred to the kinetic energy of electrons and ions. Depending on the gas, the cluster size, and pulse features, a huge variety of physical scenarios is possible, from the slow, hydrodynamic expansion of quasineutral nanoplasmas to the violent Coulomb explosion of highly charged ion clouds. The resulting ion energy is closely connected with the cluster size: for ideal spherical clusters, the theoretical maximum ion energy scales as the square of the initial radius. Large clusters (radius $\sim$10–100 nm) are, therefore, of crucial importance to obtain highly energetic ions, and have opened the way to the copious production of fusion neutrons in localized sources [2].

The diversity of physical behaviors and the interplay between the laser dynamics, the ionization dynamics, and the Coulomb explosion lead to very rich and nonlinear phenomena. An example of such phenomena was recently identified [7], predicting the occurrence of shocks [8] during the explosion of clusters with smooth (nonsteplike) profiles, in the limit of extreme vertical ionization, i.e., by assuming the laser pulse to be short and intense enough to expel all the electrons and leave a sphere of ions at rest. These conditions are quite stringent, and not easily met by large clusters. In this Letter, we show that shocks are, indeed, produced when large clusters with a steplike density profile are irradiated by an ultraintense laser; a description of shocks in this scenario requires a self-consistent treatment of the dynamics of electrons and ions in the laser field, the ionization dynamics, and the full dynamics of the explosion. We demonstrate that the electron dynamics plays an important role in the formation of the shocks for these conditions, but the shock shells are small scale, and the corresponding phase-space structure (a multiple-velocity spatial region) is tiny, so that the relative velocities inside the cluster are negligible. A technique to induce the formation of large-scale shock shells is proposed and demonstrated, based on the use of sequential laser pulses (e.g., a weak pulse followed by an ultraintense one, with a proper time delay Δt); control over the shock formation and the shock shell features can be easily attained, leading to high relative velocities inside the clusters (increasing the probability of intracluster nuclear reactions), and to the ability to tailor the properties of the ion spectrum resulting from a Coulomb explosion.

To probe these nonlinear scenarios we have performed three-dimensional (3D) and two-dimensional (2D), massively parallel, fully relativistic, electromagnetic particle-in-cell (PIC) simulations with the OSIRIS framework [9], closely matching realistic physical situations. In this code, a set of computational particles is moved under the action of their self-consistent electromagnetic field and any externally applied field: this is done by first depositing the current density on a spatial grid, then solving Maxwell's equations on the same grid and computing the force accelerating each particle, by interpolation of the field values on the position of the point particle. The numerical technique is standard PIC [10], identical to the one recently described in [11]. We have performed simulations both in the nanoplasma approximation [11,12] (substituting the target cluster with a stable cold-plasma distribution) and including self-consistent field ionization (Ammosov-Delone-Krainov) ionization model [13]). No significant qualitative differences in the physical behavior have been observed, as long as the laser intensity is high enough ($I > 10^{15}$ W/cm^2). A parameter scan was performed to guarantee the grid resolution and the size of the simulation box does not affect the results.

To motivate our discussion, we first present results from 3D PIC simulations of the interaction of an ultraintense laser pulse ($I \simeq 8 \times 10^{18}$ W/cm^2, central wavelength $\lambda_0 = 820$ nm, approximately Gaussian envelope with rise time $t_{\text{rise}} = 35$ fs) with a spherical deuterium nanoplasma (see above) (radius $R_0 = 32$ nm, uniform steplike radial density profile, $n_0 \simeq 4.5 \times 10^{22}$ cm^{-3}). The simulation box is cubic, with side $L_{\text{box}} = \lambda_0$, discretized in a $336 \times 336 \times 336$ uniform spatial grid. We employ

4.75×10^6 particles per species, a value close to the actual number of atoms, for the configuration described.

We first examine the ion density distribution, showing the outer shape of the exploding ion cloud, in Fig. 1. A shock front is already present in an early phase of the expansion, $t_a = 37.5$ fs, when the laser intensity has just started to decrease, and the few electrons in the cluster have just left the inner region, as shown by the high value of ion density in the core of the ion distribution. At a later time, $t_b = 75$ fs (the pulse has already left the simulation box), the ion density profile is almost flat in the radial direction, except for the density peak at the shock front. The outer shape of the ion cloud is slightly ellipsoidal, being elongated in the laser polarization direction, z, along which the explosion is faster [14].

Our simulations also show that the electron dynamics in the initial phase of the interaction has a crucial influence on the subsequent Coulomb explosion, as it is responsible for smoothing out the ion steplike profile, thus leading to the shock formation [7]. This smoothing out arises in the early stages of the electron expulsion and is due to the space charge field at the sharp cluster boundary, induced by the quivering motion of the electrons in the laser field. Figure 2 shows the formation and evolution of the shock shell, with the characteristic turning point in the ion $v_r - r$ phase space. The shocks still occur naturally, even when the electron expulsion time, $\tau_{el} \approx 2.7$, the shock formation time, $\tau_{shock} \approx 3.45$, and the laser rise time, $\tau_{rise} \simeq 4$, are all comparable, and the explosion does not start from a purely ion sphere. In conditions so far from the vertical ionization limit, $\tau_{el} \ll 1$, the 1D Coulomb explosion model in [7] cannot be used directly. Thus, in order to cross-check the simulation results and achieve a better comprehension of the explosion process, we used an extended version of this model, in which the electron motion is taken into account with a prescribed dynamics (that can be inferred from outer ionization models [15] or from simulations), by considering a neutralizing electron distribution whose size is gradually reduced in time according to a given law, until an only ion distribution remains. By doing so, the acceleration of an ion at a given time τ and position r can be written, in dimensionless units, as

$$\frac{d^2 r}{d\tau^2} = \frac{Q(r) - Q_{el}(r, \tau)}{r^2}, \tag{1}$$

where we normalize mass to m_i (ion mass), length to R_0 (initial cluster radius), and charge to e (elementary charge), and where the unit time $t_0 = \sqrt{(m_i R_0^3)/(e^2 N_0)}$ represents the time scale for the explosion of a pure-ion spherical distribution, N_0 being the total number of ions. The quantities $Q(r)$ and $Q_{el}(r, \tau)$ are, respectively, the ion and electron charges within a sphere of radius r at time τ. Equation (1) is integrated numerically by following the trajectory $r(r_0, \tau)$ of a finite set of ions with different initial position r_0.

In order to compare the analytical model with the simulations, we assumed the initial quasi-steplike profile $\rho_0(r_0) = 3/(4\pi)[1 - (r_0/r_{max})^\mu]$, where r_{max} is a normalization constant which provides the conservation of the total charge, with $\mu = 100$. The function $Q_{el}(r, \tau)$ is determined by lowering the outer radius of the electron distribution, $r_{el}(\tau)$, from $r_{el}(0) = r_{max}$ to $r_{el}(\tau_{el}) = 0$, following the pulse envelope evolution. Figure 2 shows the

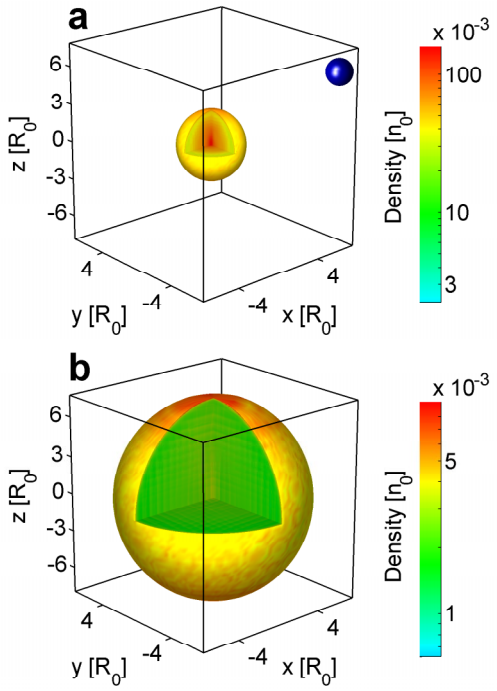

FIG. 1 (color online). Ion density distribution in configuration space at time (a) $t_a = 37.5$ fs, and (b) $t_b = 75$ fs, representing the density variation inside the ion cloud, as well as on its outer shell (where the shock front is located). As a reference, a solid sphere having the initial size of the cluster is plotted in (a). The laser pulse propagates in the x direction, and it is linearly polarized along the z direction.

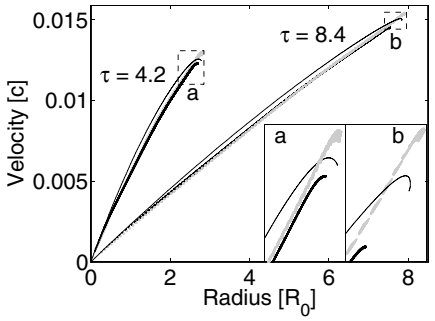

FIG. 2. Evolution of the ion phase space ($v_r - r$). Thick points represent the simulation results (black points for the y direction, and gray points for the z direction, considering the particles contained in a solid angle $\Delta\Omega \simeq 0.035$ sr around each direction); the thin lines refer to the theoretical model. Inset shows details of the small-scale shock shell in phase space. Time in units of $t_0 = 8.74$ fs.

phase space $v_r - r$ at different times, comparing the results from the PIC simulations with the results from our theoretical model. From the simulation, two curves along the y and z directions are shown, in order to illustrate the anisotropy along the polarization direction induced by the laser field. Our model neglects the complex electron dynamics in the early phase of the interaction (this may be crucial in different scenarios, for instance, when dealing with very small ($\sim$10 atoms) rare gas clusters [16], for which a self-consistent, quantum-mechanical treatment of the electron dynamics may be required for an appropriate description of the multiple ionization process), but it is very effective in describing the main features of the ion expansion, such as the time evolution for the radius of the ion cloud and the shock formation time. In the framework of this model, the shock formation time is $\tau_{\text{shock}} \simeq 3.3$, independent of our choice of μ (for large μ); this model thus provides quantitative and qualitative agreement with the simulations, and it may also be used for scenarios where the electron or ionization dynamics is more intricate, e.g., large x-ray irradiated clusters [17].

The occurrence of a shock also affects the ion kinetic energy spectrum, causing it to peak about the maximum energy value (cf. Fig. 3). The angular dependence of the energy distribution is a clear signature of the anisotropy induced by the laser field [14]: a higher ion energy is reached in the laser polarization direction, z. As a comparison, the energy spectrum $f(E) = [dQ/dr]/[vdv/dr]$ predicted by Eq. (1) is also plotted. A peak in the energy spectrum is expected as soon as a maximum in $v = dr/d\tau$ occurs (the shock predictor); such a peak is due to ions with different positions but equal velocity. The maximum ion energy is lower by 15% than the theoretical limit, $E_{\max} = (4\pi/3)q_i^2 n_0 R_0^2 \simeq 280$ keV, an estimate valid only in the ideal case of vertical ionization.

The ability to generate shock shells in the clusters opens many different directions [7], but it is also clear from single

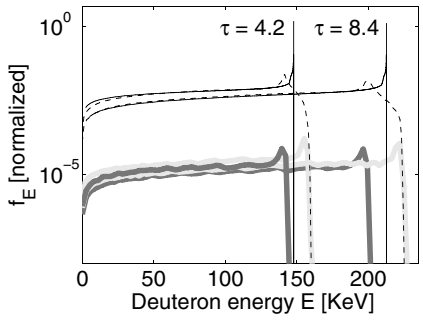

FIG. 3. Evolution of the energy spectrum. Thick lines represent the angular-dependent spectrum (dark lines for the y direction and light lines for the z direction, considering the particles contained in a solid angle $\Delta\Omega \simeq 0.035$ sr around each direction) as obtained from the simulation. Thin dotted lines represent the total energy spectrum (integrated over the solid angle); thin solid lines represent the energy spectrum from the theoretical model. Time in units of $t_0 = 8.74$ fs.

pulse simulations that only small-scale shells can be produced for realistic clusters and laser pulses. A technique to overcome this difficulty, and to produce large-scale shock shells, can be envisaged, by using sequential pulses with different intensities, namely, a weak pulse ($I \sim 10^{14}$–10^{16} W/cm^2) followed by an ultraintense pulse ($I \sim 10^{18}$–10^{20} W/cm^2), with a proper time delay Δt. The first pulse creates the plasma and heats the electrons, so that a slow, hydrodynamiclike expansion takes place [12,18] and a smoothly decreasing plasma density profile forms naturally. The second pulse removes all the electrons from the dense cluster core, causing it to explode violently and overrun the slowly expanding outer ions, thus forming a large shock shell, with considerable relative velocities inside the cluster. The main features of explosion dynamics (maximum ion kinetic energy, location of the peak in the ion energy spectrum, radial extension, and velocity spread of the shock shell) can be controlled in detail by varying the delay, Δt, between the two pulses and their intensity. This also suggests an experimental confirmation for the occurrence of shocks in clusters through the detection of time-resolved fusion-neutron bursts long before the time needed for intercluster collisions.

An estimate for the scale of Δt is readily obtained by assuming the first expansion to be purely hydrodynamic, so that its characteristic velocity is given by the ion sound speed [1,12]: $v_{\text{exp}} \sim \sqrt{(k_B T_e)/m_i}$ where $k_B T_e$ is the electron thermal energy. According to the experimental evidence [4], a large fraction ($\eta \sim 0.5$–1) of the total energy of an intense pulse can be absorbed by a gas jet of deuterium clusters within a propagation length $L \sim 1$ mm. A scaling for T_e is then simply given by $k_B T_e \sim \eta t_{\text{eff}} I/L\bar{n}$, where $\bar{n}$ is the average density of the gas jet (typically $\bar{n} \sim 10^{19}$ cm^{-3}) and t_{eff} the laser deposition time (on the order of the pulse duration). With the same laser parameters described above, but using a much lower peak intensity, $I \simeq 5 \times 10^{15}$ W/cm^2, one obtains $k_B T_e \sim 0.6$ keV, corresponding to the expansion velocity $v_{\text{exp}} \sim 1.3 \times 10^{-1}$ nm/fs. Thus, for large clusters ($R_0 \gtrsim 10$ nm), the time scale for the expansion is $\sim$100 fs. The delay Δt must be properly tuned such that the radius of the cluster increases properly ($R_{\Delta t} \sim 4 - 5R_0$) before the second pulse hits it. After the electrons are suddenly swept away from the dense cluster core, the outer ions feel a much lower Coulomb field than the inner ions do: as a consequence, a multiple-velocity spatial region is formed and the maximum relative velocity between fast and slow ions, at the same position, can be a significant fraction of the highest ion velocity ($[\Delta v/v]_{\max} \sim 0.5$), leading to collision energies up to $E_{\text{coll}} \sim 0.25 E_{\max}$. With the cluster sizes considered here, collision energies up to 100 keV are expected.

To confirm these estimates we have performed 2D simulations, in which a rodlike cluster plasma (with the same R_0 and n_0 as above) is first heated by a weak laser pulse ($I \simeq 1 \times 10^{16}$ W/cm^2, $t_{\text{rise}} = 35$ fs, $\lambda_0 = 820$ nm) and then

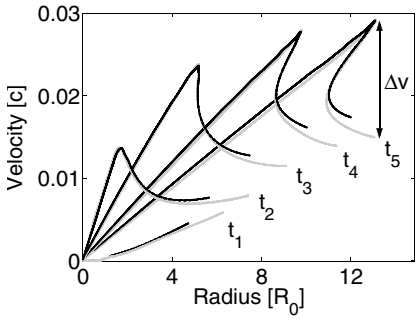

FIG. 4. Phase-space profile $(v_r - r)$ at times $t_1 = 168$ fs, $t_2 = 187$ fs, $t_3 = 206$ fs, $t_4 = 225$ fs, and $t_5 = 237$ fs. The black points refer to the x direction and the gray points to the y direction, considering the particles contained in an angle $\Delta\theta \simeq 0.1$ rad around each direction. Δv corresponds to $E_{\text{coll}} \sim 200$ keV.

torn apart by a second ultraintense pulse ($I \simeq 2.5 \times 10^{19}$ W/cm^2, $t_{\text{rise}} = 20$ fs, $\lambda_0 = 820$ nm). Both pulses propagate in the x direction, with the electric field polarized along the y direction. In this simulation, we employ $N_p \simeq 1.2 \times 10^6$ particles and a square simulation box, with side $L_{\text{box}} = 1$ μm, discretized in a 840×840 uniform spatial grid. Such a simulation describes the dynamics of a deuterium nanowire [19] irradiated by wide-spot-size laser pulses. We set $\Delta t \simeq 170$ fs: when the strong pulse comes in, the radius has expanded to $\sim 5R_0$. Figure 4 shows the time history of the phase-space profile, right after the second pulse reaches the expanding cluster. The shock shell depicts a two-knee structure, as expected for a smooth continuous initial density distribution [7]. The maximum relative velocities ($[\Delta v/v]_{\text{max}} \sim 0.5$) appear when the fastest ions, expanding in the polarization direction, z, catch up with the farthest slower ions. The 2D results also allow a comparison between 3D and 2D simulations. An estimate of the maximum collision energy in an analogous 3D case clearly points out the key differences. The ion kinetic energy is greatly overestimated in a 2D scenario, since it has no upper boundary [20], while the ratio $[\Delta v/v]_{\text{max}}$ is underestimated, since in cylindrical symmetry the electrostatic field tapers off only as $1/r$. By comparison with the 3D results presented above, we conclude that shock shells involving collision energies $E_{\text{coll}} \sim 100$ keV can actually be controlled and attainable in spherical clusters, making intracluster fusion events possible.

Though we focused on deuterium clusters, the technique presented here is general and can be applied with other cluster constituents (either one component or multicomponent) to induce specific nuclear reactions inside the clusters. For instance, with D-T clusters [21], one could tune the laser pulse sequence to obtain collision energies in the 100–150 keV range, corresponding to the maximum cross section for D-T fusion.

In conclusion, we have shown that small-scale shock shells show up naturally during the laser-induced Coulomb explosion of large deuterium clusters, even when the time scales for the electron dynamics and the ion expansion are comparable and the vertical ionization limit cannot be applied. We proposed and illustrated a method to induce large-scale shock shells, thus providing the ability to fully control the key features of the ion dynamics in laser-irradiated clusters, and to induce intracluster nuclear reactions.

The authors thank M. Marti, Professor W. B. Mori, Professor G. Coppa, Dr. A. D'Angola, Dr. M. Fajardo for discussions, and S. Martins for the development of the OSIRIS ionization module. This work was partially supported by FCT (Portugal) through Grants No. POCTI/FAT/43743 and No. POCTI/FAT/49540.

*Electronic address: luis.silva@ist.utl.pt

[1] V. P. Krainov and M. B. Smirnov, Phys. Rep. **370**, 237 (2002).
[2] T. Ditmire *et al.*, Nature (London) **386**, 54 (1997); T. Ditmire *et al.*, Nature (London) **398**, 489 (1999); J. Zweiback *et al.*, Phys. Rev. Lett. **84**, 2634 (2000); J. Zweiback *et al.*, Phys. Rev. Lett. **85**, 3640 (2000); T. Ditmire *et al.*, Phys. Plasmas **7**, 1993 (2000); K. W. Madison *et al.*, Phys. Plasmas **11**, 270 (2004); G. Grillon *et al.*, Phys. Rev. Lett. **89**, 065005 (2002).
[3] I. Kostyukov and J.-M. Rax, Phys. Rev. E **67**, 066405 (2003); I. Y. Kostyukov and J.-M. Rax, Phys. Rev. Lett. **83**, 2206 (1999).
[4] T. Ditmire *et al.*, Phys. Rev. Lett. **78**, 3121 (1997).
[5] K. Y. Kim *et al.*, Phys. Rev. Lett. **90**, 023401 (2003).
[6] I. Last and J. Jortner, Phys. Rev. Lett. **87**, 033401 (2001).
[7] A. E. Kaplan *et al.*, Phys. Rev. Lett. **91**, 143401 (2003).
[8] G. B. Witham, *Linear and Nonlinear Waves* (Wiley, New York, 1974).
[9] R. G. Hemker, Ph.D. thesis, UCLA, 2000; R. A. Fonseca *et al.*, in *Lecture Notes in Computer Science* (Springer-Verlag, Heidelberg, 2002), Vol. 2329, p. III-342.
[10] C. K. Birdsall and A. B. Langdon, *Plasma Physics via Computer Simulation* (McGraw-Hill, New York, 1985).
[11] C. Jungreuthmayer *et al.*, Phys. Rev. Lett. **92**, 133401 (2004).
[12] T. Ditmire *et al.*, Phys. Rev. A **53**, 3379 (1996).
[13] M. V. Ammosov *et al.*, Sov. Phys. JETP **64**, 1191 (1986).
[14] V. Kumarappan *et al.*, Phys. Rev. Lett. **87**, 085005 (2001); M. Krishnamurthy *et al.*, Phys. Rev. A **69**, 033202 (2004).
[15] I. Last and J. Jortner, J. Chem. Phys. **120**, 1336 (2004); **120**, 1348 (2004); P. B. Parks *et al.*, Phys. Rev. A **63**, 063203 (2001).
[16] M. Brewczyk *et al.*, Phys. Rev. Lett. **80**, 1857 (1998); I. Grigorenko *et al.*, Europhys. Lett. **57**, 39 (2002).
[17] R. Neutze *et al.*, Nature (London) **406**, 752 (2000); H. Wabnitz *et al.*, Nature (London) **420**, 482 (2002); U. Saalmann and J.-M. Rost, Phys. Rev. Lett. **91**, 223401 (2003).
[18] M. Lezius *et al.*, Phys. Rev. Lett. **80**, 261 (1998); H. M. Milchberg *et al.*, Phys. Rev. E **64**, 056402 (2001); C. S. Liu and V. K. Tripathi, Phys. Plasmas **10**, 4085 (2003).
[19] A. C. Dillon *et al.*, Nature (London) **386**, 377 (1997).
[20] Y. Kishimoto *et al.*, Phys. Plasmas **9**, 589 (2002).
[21] I. Last and J. Jortner, Phys. Rev. A **64**, 063201 (2001).